A computational simulation of neuromuscular block monitor sensitivity to procedural variability

Ryan Spears, Taylor Tew, and Katie Carroll

Introduction

In the United States, there are 51.4 million inpatient surgeries annually, 50% of which require the use of neuromuscular blocking agents (NMBAs) [1]. Neuromuscular block is the drug-induced systemic inhibition of chemical transmission across the neuromuscular junction, reversibly paralyzing skeletal muscle throughout the body. NMBAs are used in conjunction with general anesthesia to prevent unwanted muscle activity in the sedated patient that can interfere with operations, most commonly intubation [2]. When NMBAs are used, monitoring the degree of neuromuscular block is vital. Too little block can fail to prevent block interfering muscle contractions that can disrupt an operation while too much block can leave residual agent in the body, leading to complications such as intensive care unit-acquired weakness that can have serious health consequences, especially on respiratory function [3].

Traditional monitoring uses a two-electrode peripheral nerve stimulator to apply current at the wrist to the ulnar nerve, which a clinician then assesses via tactile and visual assessment of adductor pollicis deflection, providing a qualitative, subjective indicator of the degree of block. The emerging standard of care replaces the clinician assessment with an electromyographic sensing system over the adductor pollicis, providing a quantitative, objective measure of the degree of block [4]. Both systems use a train-of-four (TOF) stimulation pattern, which consists of four 300μs constant-current square pulses applied at 2Hz. Current thresholds, which can range from 5-60mA at 5mA intervals, are established before anesthetics and NMBAs are applied, and then stimulation is applied at the established threshold level periodically throughout the procedure.

A common clinical observation in using these systems is that the current required for use is greater for patients with more subcutaneous fat, though there is uncertainty whether the relationship is causative or correlative. Because the threshold is established before anesthetics are applied, too high a current can activate sensory fibers in the ulnar nerve and result in pain in the patient. It is therefore important to keep current thresholds as low as possible not just to minimize power consumption, but to ensure patient comfort.

Three factors likely contribute to the observed effects: (1) increased fat increases the normal distance between the electrode and the nerve fiber, increasing current thresholds in line with a standard strength-distance relationship, (2) the insulative properties of the fat attenuate current flow, and (3) subcutaneous fat obscures surface markers used to place electrodes, making inaccurate placement in the coronal plane more likely, increasing thresholds in line with a standard strength-distance relationship. In a clinical setting, controlling the variables needed to distinguish between these factors would be difficult, especially the insulative properties of fat and the normal strength-distance relationship. A computational model, however, can precisely control these variables. This study will seek to use such a model to determine the relative contribution of these three factors to the clinical observation that increased levels of subcutaneous fat correspond to increased current thresholds.

Methods

COMSOL

The purpose of the COMSOL model was to reveal changes in the distribution of tissue voltages due to the manipulation of subcutaneous fat thickness and lateral electrode-to-nerve distance. The geometry is modeled using three-dimensional blocks for the skin (0.08 inch thickness), subcutaneous fat (varying thickness 0.1-1.0 inch), and muscle (4 inch thickness).

Each layer material had a characteristic conductivity σ and permittivity ϵ_r based on validated values [5, 6]. Utilizing the quasistatic approximation, the model was assumed to be time independent.

***Table 1**: Material properties used in the COMSOL model*

Material	σ **(S/m)**	ϵ_r
Muscle [5]	0.333	40000
Fat [5]	0.03	25000
Skin [5]	0.00025	6000
Electrode Interface (Hydrogel) [6]	0.0033	1

A DC current stimulated the model to find the voltage distribution of the tissue at a given pulse input. The mesh was refined until no significant changes in voltage distribution were found. The nerve voltage was read at a constant distance of z = 3.6 in, shown as the red line in Figure 1. As subcutaneous fat thickness increased, the electrode-to-nerve fiber distance increased equivalently. The 0.5 inch electrode interfaces were placed 1 inch apart, corresponding to the standard testing procedure.

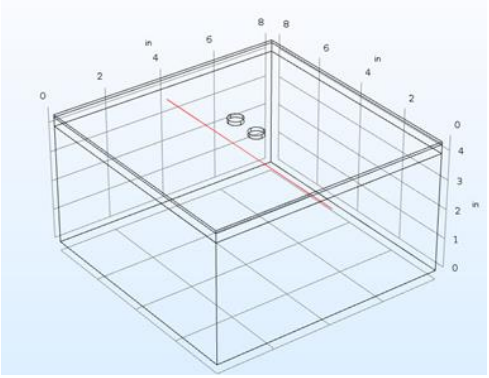

***Figure 1**: Nerve positioned in the 3D tissue model.*

To validate the use of COMSOL Multiphysics, the experimental voltage distribution given by a point source was compared to the analytical solution determined by the equation:

$$V = \frac{I}{\sigma \pi r} \qquad [1]$$

where $I_1 = 50\ mA$, $I_2 = -50\ mA$ and $\sigma = 0.05$ S/m. To ensure that the medium is large enough as to not be affected by the ground boundary condition, a comparison was conducted.

***Table 2**: Comparison of voltage distribution between the experimental and analytic point source*

Point (x,y,z)	Experimental (COMSOL) (V)	Analytical (V)	% Difference
-3, 1, 1	1.668	1.700	1.88%
-1, 0.5, -0.5	0.6928	0.6997	0.98%
0,0,0	5.022E-5	0	0%
-0.5, -0.5, -0.75	0.3054	0.2928	4.30%
4, 0, 0	-2.6300	-2.6854	2.06%

Next, we ensured that the ground boundary conditions did not affect the exported voltage from the 3D tissue model. To test this, the volume was increased in both the x, y, and z-directions 1 inch until there was <1% change in maximum voltage along the model nerve at a stimulus of 45 mA. Table 3 shows the results of the validation:

***Table 3**: Ground boundary validation along each 3D axis*

	X-Coordinate	Y-Coordinate	Z- Coordinate
Change in Voltages (V)	-0.0082	-0.0032	-0.0117
% Difference	.4686%	.1825%	.6727%

MATLAB & NEURON

A simple NEURON model of a single efferent axon of an alpha motor neuron was created to simulate the effects of stimulation. The axon, which was assumed to have Hodgkin-Huxley membrane dynamics, was 20µm in diameter and 20.1cm in length (12.7cm from distal electrode to axon terminal). Voltages exported from the 3D tissue model did not have regular axial spacing due to the mesh composition and therefore required processing

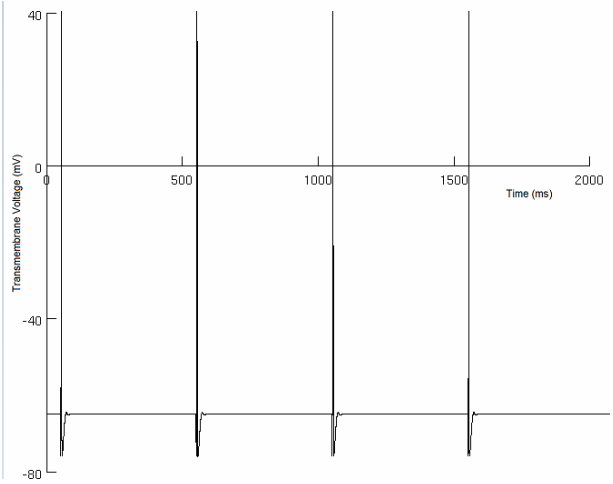

***Figure 2**: Membrane response to a train-of-four stimulus applied at suprathreshold current.*

prior to being input into a physiologic model. The potentials were interpolated at 2mm apart to obtain extracellular voltages at internodal distances of 100*diameter. These potentials were then exported to the NEURON model and inputted as extracellular voltage sources at each node along the length of the axon in a TOF pulse sequence. The potentials at the end node were then taken to be representative of the potentials at the neuromuscular junction.

Testing

Slight parameter shifts were performed in COMSOL to help determine the relationship between subcutaneous fat thickness, lateral electrode positioning to the nerve, current stimulation, and nerve depth. Current amplitudes of stimulation were increased until an action potential occurred for all fat thicknesses and lateral electrode positions to obtain a table of binary action potential results. The thickness of subcutaneous fat was increased from 0.1 inch to 1 inch while using a constant current stimulus of 5.0 mA and constant lateral electrode distance of 0.3 inches to help visualize the results of varying the fat thickness on the magnitudes of the second differences in extracellular potential.

The lateral electrode distance was increased from 0 inches (i.e. directly underneath the center of the electrode) to 1 inch from the center while using a constant current stimulus of 3.75 mA and constant fat thickness of 0.3 inches to help visualize the results of varying the lateral electrode distance on the magnitudes of the second differences in extracellular potential. To evaluate the degree of second difference voltage contribution between electrode-to-fiber depth and fat thickness, nerve depth was alternately increased by first repositioning the nerve deeper into the muscle and second varying fat thickness. By comparing the magnitudes of the second difference, the degree of contribution between the electrode-to-fiber depth and varying fat thickness can be evaluated.

Results

Varying current amplitude

Figure 3 shows the result of a simulation at 0.3 inch fat thickness with the lateral electrode distance 0.3 inches from the nerve. Holding these variables constant and increasing the current stimulus produced a larger second difference in extra-cellular voltage.

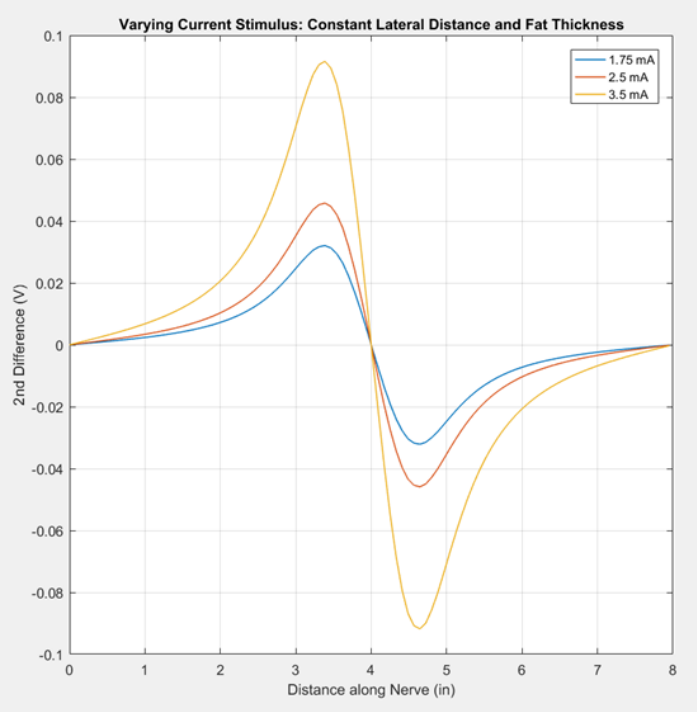

***Figure 3**: Second differences of extracellular voltage along the length of the axon for three current amplitudes.*

Varying subcutaneous fat thickness

Figure 4 displays the results of varying the thickness of subcutaneous fat with a constant electrode position of 0.3 inches lateral to the nerve fiber and a constant 5 mA stimulus. The data shows that patients with larger fat thicknesses require more current stimulation to obtain the same magnitude of second differences in extracellular potential. Also, the normalized plot shows there was an enhanced distribution of second difference in extracellular potential along the length of the nerve fiber.

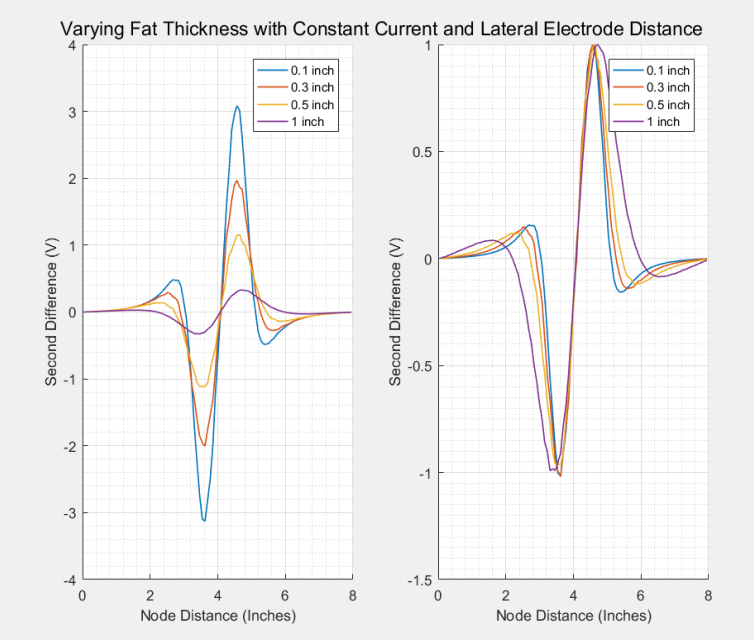

***Figure 4**: Second differences of extracellular voltage along the length of the axon for four fat thicknesses, unnormalized (left) and normalized (right).*

Varying lateral electrode position

Figure 5 below shows the results of a simulation run at 0.3 inch fat and a constant current stimulus of 3.75 mA with varying lateral electrode distance. The results show a decreased magnitude of second difference voltage as the lateral electrode-to-nerve distance is increased.

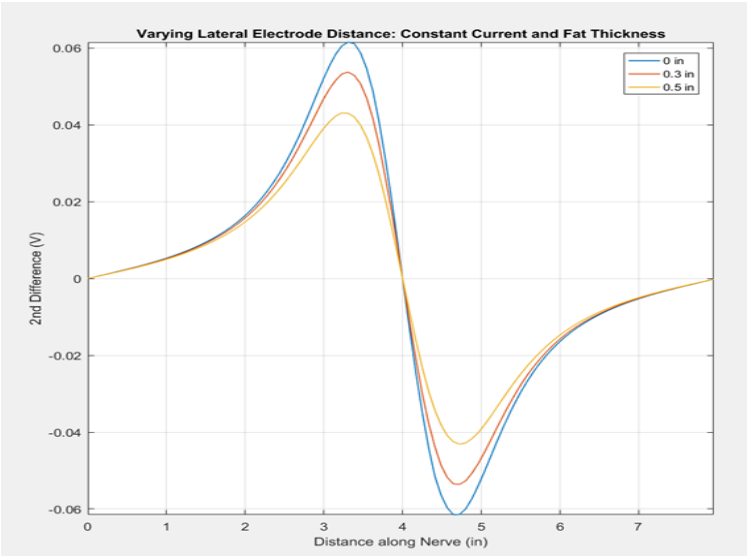

***Figure 5**: Second differences of extracellular voltage along the length of the axon for three lateral electrode positions.*

Figure 6 summarizes the effects of fat thickness, lateral electrode position and current stimulus magnitude on generating an action potential, showing that as fat thickness and lateral electrode distance increase, the current threshold for activation increases.

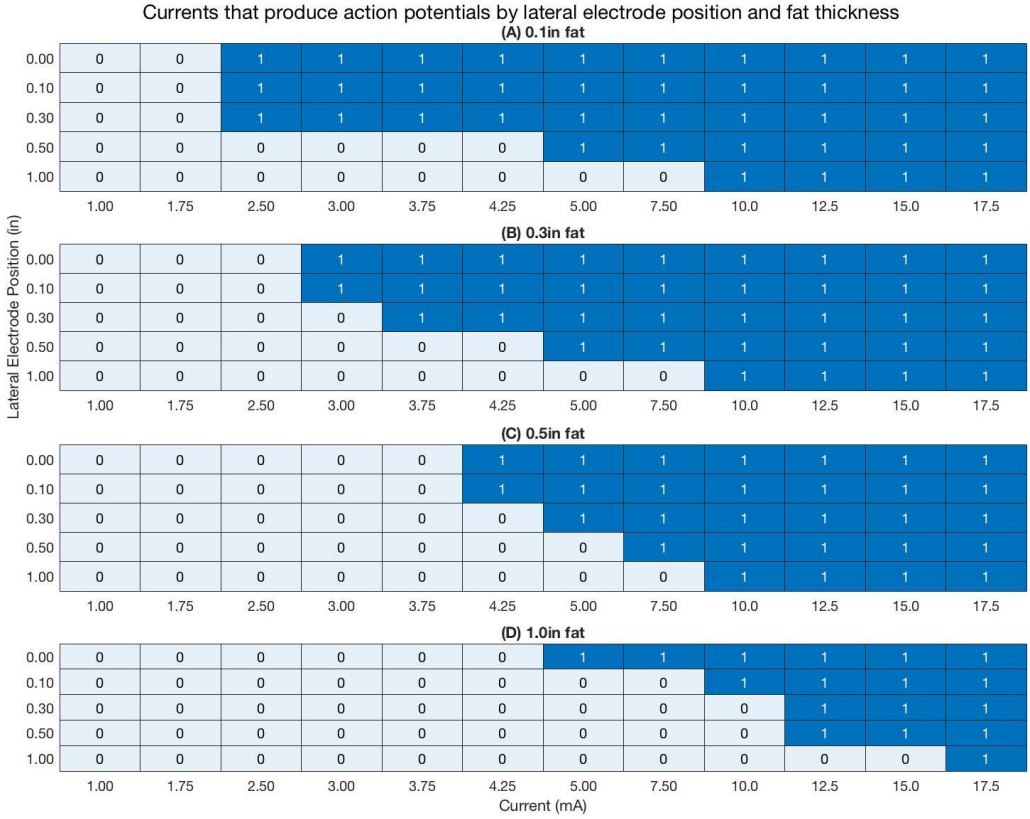

***Figure 6**: Binary chart of action potential generation over twelve stimulation current amplitudes, five lateral electrode positions, and four fat thicknesses. 0 indicates no action potential occurred, and 1 indicates an action potential did occur.*

Comparing varied fiber depth to varied fat thickness

The purpose of Figure 7 is to distinguish the effects of fat thickness and electrode-to-fiber distance in increasing current activation thresholds. The constant fat thickness graph (top) holds the fat thickness at 0.1 inches and increases the electrode-to-fiber distance by lowering the nerve depth location and increasing the fat thickness so that the overall electrode-to-nerve distance is

second difference voltages from the variable fat thickness second difference voltages, isolating the effect of the fat material. Within physiological bounds, fat has a minimal amplification effect on the second difference extracellular voltage. The waveforms representing 0.285 inch electrode-to-fiber distance are the same simulation in all three subplots and therefore act as a control in calculating the impact of fat thickness to electrode-to-fiber distance.

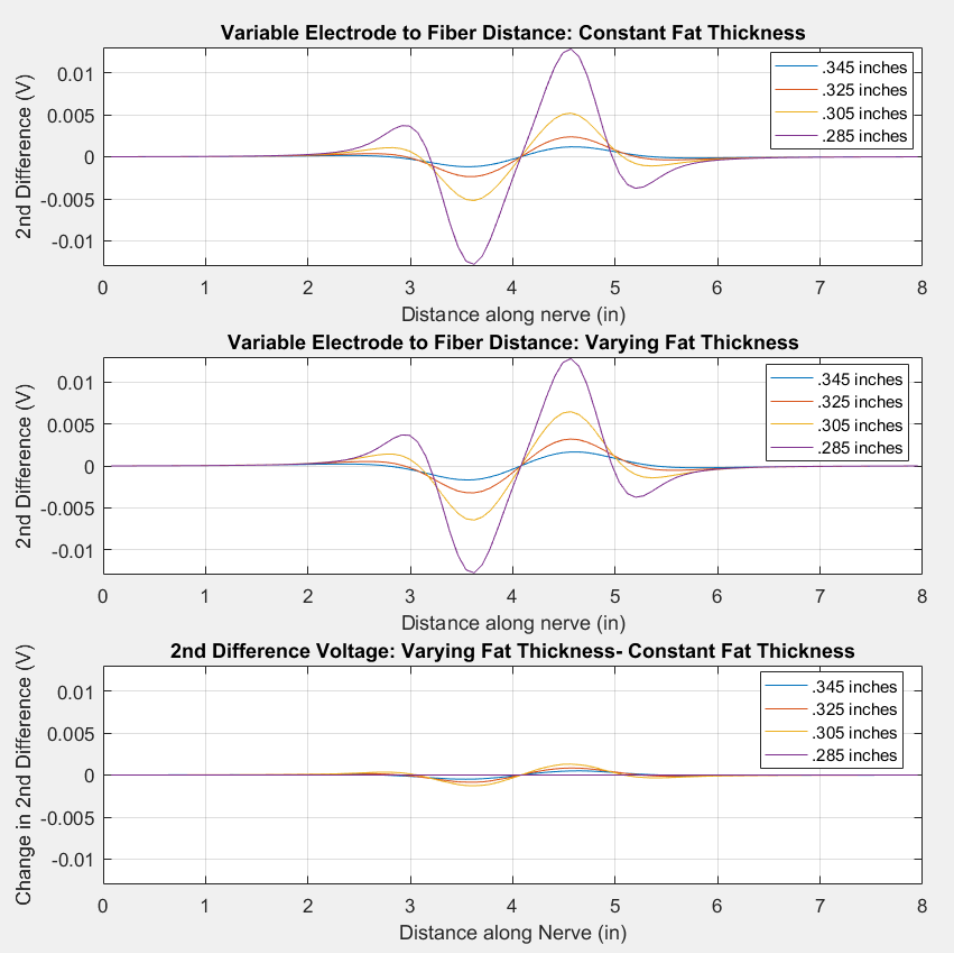

***Figure 7**: Second differences of extracellular voltage along the length of the axon for four electrode-to-fiber depths with fat thickness kept constant (top) and varied equivalent to the change in depth (middle). The contribution of fat thickness to the second differences (bottom) was isolated by taking the difference of the second differences generated with constant fat thickness and varied fat thickness.*

The following equation was used to calculate the ratios in Figure 8, where V_c is constant fat thickness voltage, Vv_f is variable fat thickness voltage and n is distance of interest:

$$ratio = \frac{V_{c,0.285} - V_{c,n}}{V_{f,n} - V_{c,n}} \quad [2]$$

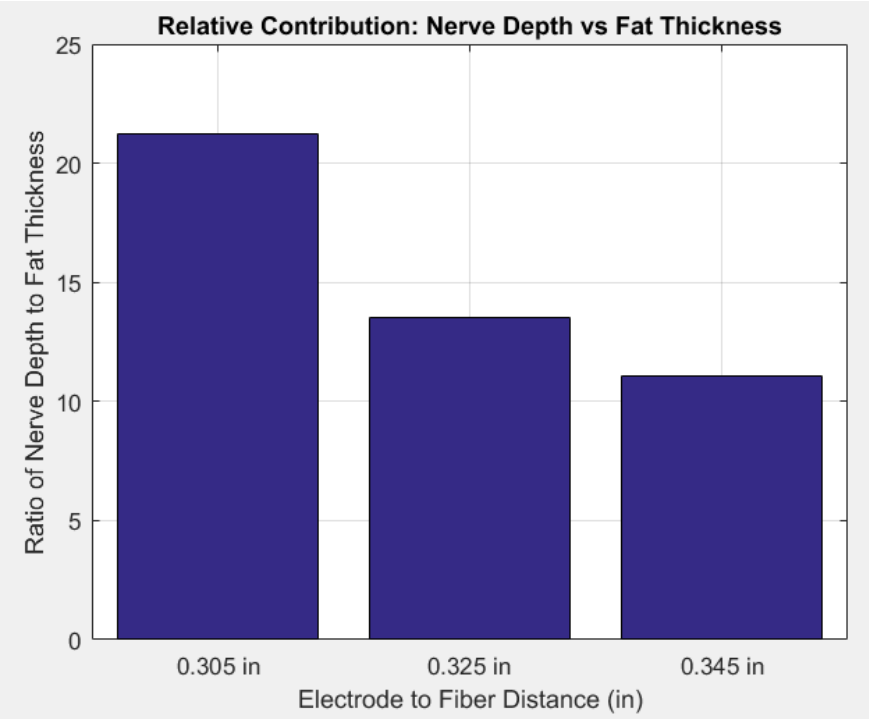

***Figure 8**: The relative contribution of electrode-to-fiber depth and fat thickness to second differences of extracellular voltage along the length of the axon, as described mathematically in equation 2. A value greater than 1 indicates predominance of electrode-to-fiber distance, and a value less than 1 indicates the predominance of fat thickness.*

Discussion

Extracellular second difference voltage values increased with current stimuli when fat thickness and lateral electrode-to-fiber distance were held constant (Figure 3). This correlated to increased magnitude extracellular sources along the nerve, and therefore, we expect a larger stimulus to more frequently induce action potentials.

An increase in subcutaneous fat thickness decreased the second differences of extracellular potentials when a stimulus amplitude and lateral distance to the nerve were held constant (Figure 4). NEURON simulations confirmed that decreased second differences resulted in increased current activation thresholds for action potentials. This correlated with smaller

current stimuli inducing action potentials in patients with 0.1 inch fat thickness versus 0.5 inch fat thickness.

An increased lateral electrode-to-nerve distance reduced the second differences in extracellular voltage values when fat thickness and current stimuli were held constant (Figure 5). This corresponded with the electrode-to-fiber distance to current threshold relationship in which a larger electrode-to-fiber distance required a larger stimuli to achieve an action potential.

Figure 7 shows that both electrode-to-fiber distance and fat thickness have an effect on the second difference voltages. Increasing fat thickness slightly increases the second difference voltages, with the effect more pronounced for smaller electrode-to-fiber distances than larger distances. The ratios shown in Figure 8 are much greater than one, so we therefore conclude that electrode-to-fiber distance has a substantially greater impact on second difference voltages than the increased presence of fat.

The COMSOL model can be refined to assess differential electric fields through the nerve more accurately. In this simple model, materials were assumed to be isotropic and homogeneous. In future iterations, increasing the complexity of the material and nerve orientation/position can create more realistic physiological results. The primary path for improving the model, though, is making the NEURON component more representative of the anatomic system. More elements do not necessarily need to be added, but incorporation of motor units and motor pools would account for variable innervation of muscle fibers, taking the system from a binary representation of muscle activation to a graded representation more indicative of the motor output acquired with electromyography. Introduction of calcium dynamics would also more accurately correspond to neurotransmitter release, though calcium flux is proportional to

transmembrane potential, so such dynamics are not strictly needed to assess activity at the neuromuscular junction.

A parallel clinical study would also be desirable to provide a controlled corollary for comparison. Patients would not need to receive anesthetic or NMBA, as thresholds are established before either are applied. Imaging techniques such as ultrasound could potentially be used to control electrode placement and measure subcutaneous fat content. Parameters for grouping patients by subcutaneous fat content would need to be established. Thresholds would be acquired for each patient with varying lateral electrode positions, with measurements ideally repeated in each individual. Comparison would be performed within patients for the effect of lateral electrode position and between groups for the effects of subcutaneous fat content.

References

1. Thompson JS, Baxler BT, Allison JG, Johnson FE, Lee KK, and Park WY. Temporal patterns of postoperative complications. *Arch Surg.* 138.6:596-602, 2003.
2. Appiah-Ankam J, and Hunter JM. Pharmacology of neuromuscular blocking drugs. *Continuing Education in Anaesthesia Critical Care & Pain*. 4.1:2-7, 2004.
3. Sessler CN. Train-of-four to monitor neuromuscular blockade? *CHEST Journal.* 126.4:1018-1022, 2004.
4. Brull SJ, Renew JR, and Neguib M. Monitoring neuromuscular blockade. UpToDate. [updated Nov 2017]. https://www.uptodate.com/contents/monitoring-neuromuscular-blockade.
5. Kuhn A, and Keller T. A 3D transient model for transcutaneous functional electrical stimulation. International Functional Electrical Stimulation Society Conference, 2005.
6. Kuhn A. Modeling transcutaneous electrical stimulation, PhD thesis, Swiss Federal Institute of Technology (ETH) in Zurich, Switzerland. https://www.researchcollection.ethz.ch/bitstream/handle/20.500.11850/150646/eth-30794-02.pdf.